JACS
JOURNAL OF THE AMERICAN CHEMICAL SOCIETY
Article
pubs.acs.org/JACS

Water Oxidation Mechanism for Synthetic Co−Oxides with Small Nuclearity

Xichen Li and Per E. M. Siegbahn*

Department of Biochemistry and Biophysics, Arrhenius Laboratory, Stockholm University, SE-106 91 Stockholm, Sweden

Supporting Information

ABSTRACT: Hybrid DFT model calculations have been performed for some cobalt complexes capable of oxidizing water. Since a very plausible mechanism for the oxygen-evolving complex involving the cuboidal Mn_4Ca structure in photosystem II (PSII) has recently been established, the most important part of the present study concerns a detailed comparison between cobalt and manganese as water oxidation catalysts. One similarity found is that a M(IV)−O$^{\bullet}$ state is the key precursor for O−O bond formation in both cases. This means that simply getting a M(IV) state is not enough; a formal M(V)═O state is required, with two oxidations on one center from M(III). For cobalt, not even that is enough. A singlet coupled state is required at this oxidation level, which is not the ground state. It is shown that there are also more fundamental differences between catalysts based on these metals. The favorable low-barrier direct coupling mechanism found for PSII is not possible for the corresponding cobalt complexes. The origin of this difference is explained. For the only oxygen-evolving cubic Co_4O_4 complex with a defined structure, described by Dismukes et al., the calculated results are in good agreement with experiments. For the Co_4 models of the amorphous cobalt−oxo catalyst found by Nocera et al., higher barriers are found than the one obtained experimentally. The reasons for this are discussed.

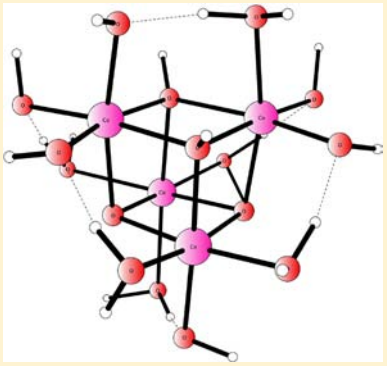

1. INTRODUCTION

Photosystem II (PSII) is the only system in nature that catalyzes water oxidation into dioxygen, protons, and electrons. During the past decade the understanding of the structure[1−4] and the O−O bond formation mechanism[5] has increased rapidly, where theoretical studies using density functional theory have played a major role. At present, it can even be claimed that a detailed knowledge of all the steps leading to O_2-formation and release is quite close.[6−8] Further references to the large amount of experimental and theoretical work done on the PSII mechanism can be found in recent reviews.[6,9−11] The catalyst is the so-called oxygen-evolving complex (OEC), which has a cuboidal structure with a Mn_4Ca metal unit, connected by oxo bonds. In parallel to the work on the natural system, there has been, during recent years, an increased effort in making synthetic systems that can perform the same task. The information gathered on how nature has solved the problem of utilizing sunlight and abundant metals in an efficient way should be of significant importance in this context. In the present study, the class of cobalt−oxide complexes have been investigated by model calculations, and the mechanisms obtained are compared to the one in PSII.

About 5 years ago, the group of Nocera et al found an amorphous cobalt−oxide catalyst that has generated considerable interest.[12] The catalyst is self-healing and functions at neutral pH. The active catalyst is believed to be formed of clusters of various sizes. EXAFS studies indicate a cuboidal structure with a Co_4O_4 building unit (CoO_6 edge-sharing octahedra),[13,14] interestingly similar to the Mn_4Ca unit of the OEC. However, the turnover rate of this catalyst is several orders of magnitude slower than the one of PSII,[15] which means that further work to improve the efficiency should be possible.

Dismukes et al recently found another interesting cobalt complex found to evolve oxygen. The structure of this molecular complex has been determined showing that it also has a cuboidal Co_4O_4 metal unit similar to the OEC.[16] Since a complex with one less cobalt did not evolve oxygen,[17] it was suggested that having the full cubic structure of the complex should be a significant factor for catalysis. There are recent reviews where further references to cobalt catalysts can be found.[18,19]

The first synthetic molecular water oxidation catalyst, the so-called blue dimer, was found by Meyer et al.[20] It consists of a ruthenium dimer with a bridging oxo, and with bpy ligands. The Llobet catalyst is one among many other ruthenium catalysts found later.[21] The blue dimer and the Llobet catalyst were recently compared using the present DFT approach.[22] Licheng et al,[23] found the most efficient molecular catalyst to date, with a rate approaching that of PSII. Further references to the vast amount of similar biomimetic work can be found in recent reviews.[18,21,24]

There has only been one earlier theoretical study trying to identify the O−O bond formation mechanism of the Nocera catalyst.[25] As a starting point for the studies, the simplest

Received: May 28, 2013
Published: August 22, 2013

   dx.doi.org/10.1021/ja4053448 | J. Am. Chem. Soc. 2013, 135, 13804−13813

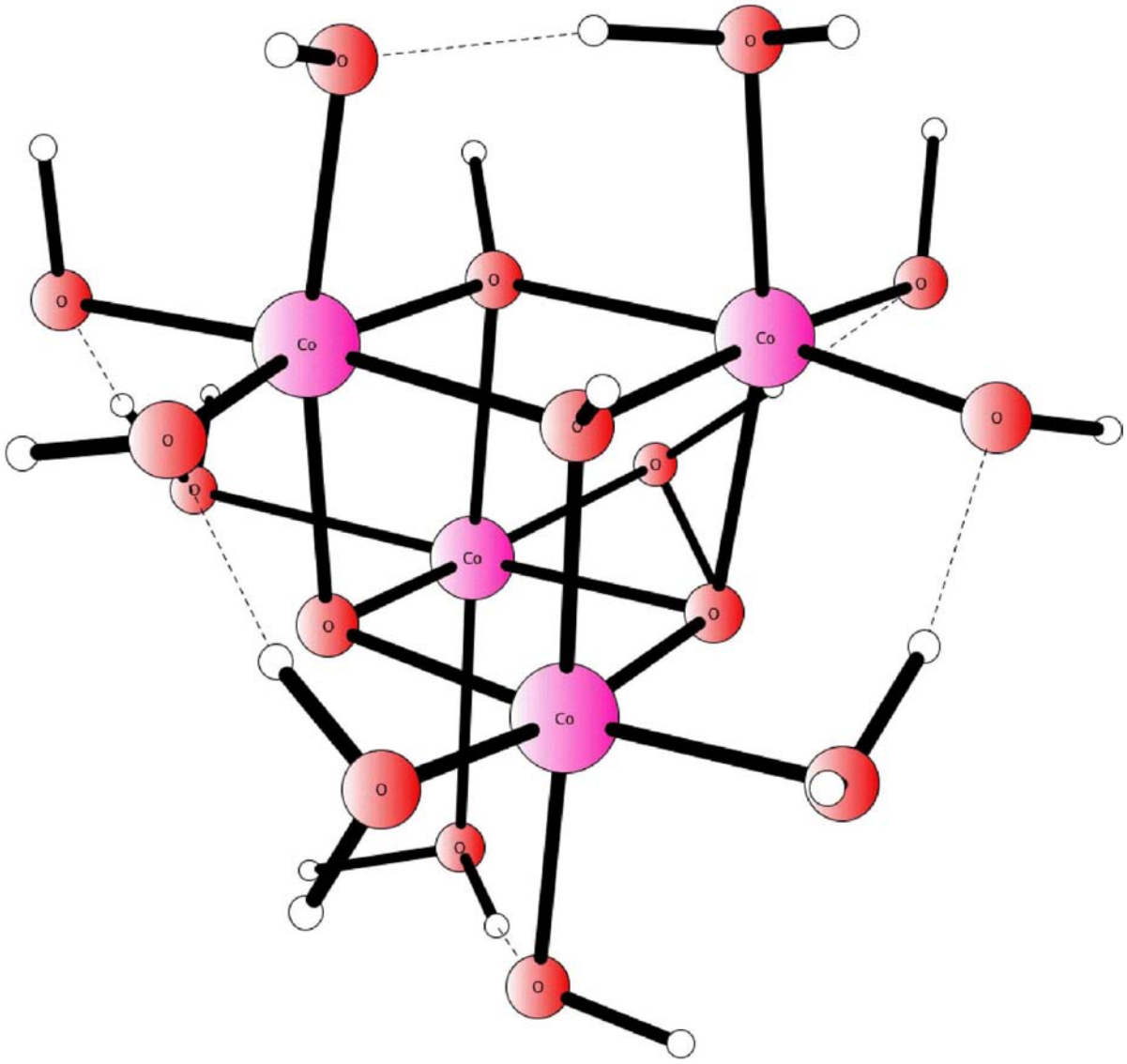

Figure 1. Optimized structure for the neutral Co_4-model where all metals are Co(III).

possible neutral complex was used with only water-derived ligands. The same approach is used here, since the phosphates in the actual catalyst are not believed to be significant for the O−O bond-formation step.[26] This conclusion was derived from a zeroth-order dependence of the kinetics on the concentration of the phosphate. Additional calculations performed have shown that, when a water was replaced by a HPO_4^{2-}, there was no significant effect on the O−O bond-formation barrier. Furthermore, in previous studies on PSII, it has been found that substituting the actual ligands by water-derived ligands (carboxylates by hydroxides and histidine by water) did not have any qualitative effect on the mechanism.[5] Although the model is seemingly simple, there are many more investigations that can be made with this model. One important remaining question is to find the optimal protonation state of the model complex at all stages. In fact, the optimized structure in the present study for the all-Co(III) complex is over 40 kcal/mol more stable than the one used in the previous study, see further below. It is estimated that around 2000 configurations/conformations/spin states have been investigated in the present two-year study. In the case of PSII, it has been demonstrated that finding the structure with the lowest energy is absolutely essential for finding the correct mechanism.[27] Another difference from the previous study is an investigation of what happens when the Co_4O_4 metal unit is modified by removing or adding one cobalt. A third one is a determination also of the redox steps of the catalytic cycle. With these additional investigations performed here, the suggested mechanism is quite different from the one of the previous study.

To understand water oxidation, the steps where electrons and protons leave have to be explicitly treated. The strategy for obtaining information about these latter steps is the same as has been successfully used for studies of water oxidation in PSII and proton pumping in cytochrome oxidase, among others.[4,28,29] In addition, the mechanism has also been investigated for the cubic Co_4O_4 complex found by Dismukes et al.[16]

The present study is also a starting point for a systematic investigation of mechanistic differences between homogeneous and heterogeneous catalysts for water oxidation. Two homogeneous catalysts with a ruthenium dimer have been studied with the present methods before.[22] The somewhat larger OEC complex in PSII has been well studied.[6] A

dx.doi.org/10.1021/ja4053448 | J. Am. Chem. Soc. 2013, 135, 13804−13813

comparison of the thermodynamics of the natural PSII catalyst with heterogeneous metal−oxo catalysts has also been done,[30] where similarities between the two types of catalysts were pointed out. A remaining question is whether the actual O−O bond-formation mechanisms also have similarities. The results obtained so far for homogeneous catalysts indicate that an oxygen radical is required for a low barrier for O−O bond formation. The most common view is that for heterogeneous catalysts the position of the Fermi level is the critical issue, which might indicate that the mechanism could be quite different in character than for homogeneous catalysts. The present amorphous cobalt−oxo catalyst represents an interesting intermediate case, which could give further insight into the heterogeneous mechanism.

2. METHODS AND MODELS

In the calculations performed here, the B3LYP* functional with 15% exact exchange[31] (rather than 20% as in the original B3LYP functional) was used, because of its superior performance in most cases for describing transition metal redox reactions.[4−6] In order to test the stability of the DFT functional for the present biomimetic systems, the results with 15% and 20% exchange were compared. The results for the chemical steps were found to be quite similar with differences of only 2−3 kcal/mol. For the redox steps the differences are larger, but since these energies are fitted to the experimental driving force, these differences are of minor importance. The DFT energies reported here should thus be reasonably stable. The energetics was obtained using large, nearly saturated basis sets (cc-pvtz(−f), lacv3p+) in single-point calculations at geometries optimized using a smaller basis set (lacvp*). Solvation effects were calculated using the standard PBF solvent model in *Jaguar*.[32] The dielectric constant was chosen as 81.0, and a probe radius of 1.4 Å was used. Zero-point vibrational effects were calculated using the lacvp* basis set. All these calculations were done using the *Jaguar* program, except for the transition state optimizations and frequency calculations, which were performed using the *Gaussian* program.[33]

The procedure to set up energy diagrams is the same as in previous studies on photosystem II, cytochrome oxidase, and the ruthenium catalysts.[4,28,29,22] In essence, the relative energies calculated are assumed to reasonably accurately reflect the *relative* redox and pK_a values. The results of the calculations are then fitted to reproduce the experimental exergonicity of the reaction, given by the experimental redox potentials of the electron donor (H_2O) and acceptor at the given pH. The energies for the releases of the (H^+,e^-)-couples in the redox accumulation part are uniquely determined by this exergonicity and the calculated relative energies. Because the system after the release of a (H^+,e^-)-couple maintains its charge, the effect of the surrounding will be small and should be well described by the dielectric cavity model. To determine the individual redox and pK_a values, where the surroundings play a major role, a single empirical parameter has to be introduced. Since in the present case there are no experimentally determined energies to compare to, only the thermodynamics of the releases of the (H^+,e^-)-couples are reported. The kinetics for these redox steps cannot be reliably computed using the present models and are here assumed to be rather fast and not rate-limiting, which has been supported by experiments on these systems.[26] However, this has been shown not always to be the case.[34] For a nickel-containing catalyst the rate was in fact dependent on the PCET steps involving the buffer.

The binding of a H_2O molecule to the surrounding water medium can give large errors for limited models. In the energy diagrams presented below, an empirical value of 14 kcal/mol has therefore been used (the same as in the previous studies), taken from experience from numerous applications. In the case of the binding energy of an O_2 molecule, a gain of entropy of 12 kcal/mol is used as an approximate value for releasing it from a metal complex to the gas phase. Apart from that case, the entropy effects were found to be small (less than 2 kcal/mol) when the topology remained but can be as large as 6 kcal/mol when there were topological changes. For example, in the O−O direct coupling pathway for the Co_3 model, the entropy effects increased by 6 kcal/mol after O−O bond formation. Zero-point effects were included and are quite large for proton release steps. This procedure for entropy and zero-point effects was used to be compatible with the calculations on photosystem II, which were done in that way. The energies in the diagrams can be regarded as free energies.

It has recently been realized that dispersion effects, neglected in DFT, could give significant contributions for metal complexes.[35] In the present study these are therefore added using the empirical formula of Grimme.[36] This formula depends only on the geometric and not on the electronic structure. With a cutoff for short distances, the dispersion contribution depends on the number of distances of intermediate size in the structure. This means that, when molecules are added, such as water, there will be an increase of dispersion and a decrease when molecules, such as O_2, leave. With the addition of dispersion and the use of 15% exchange, most of the known main failures of B3LYP for transition metal systems have been eliminated.

The optimized models used here for the amorphous cobalt oxide were built empirically, see Figure 1, because no experimentally determined structures exist. It should be noted that one second shell water molecule has been added for all complexes since it is needed in the water attack mechanism. This water was checked for all structures and was removed from that structure when its binding energy was less than 14 kcal/mol. In that case it is better bound in the water medium surrounding the catalyst, which is not included in the model, and its energy is taken to be 14 kcal/mol.

In the present type of investigation, it is very important to search for the lowest energy state by looking at all possible protonation states and spin combinations. However, in order to focus on the results of main interest, all these details have been given only as ESI.

3. RESULTS AND DISCUSSION

The Results and Discussion section will be divided into three subsections. The regular Co_4O_4 model cluster will be discussed first, since it has been found to be the main building block of the Nocera catalyst. However, the water oxidation mechanism can also be associated with edges and defects of the catalyst. Models where one cobalt was either removed or added were therefore also studied with results presented in section 3.2. As mentioned in the Introduction, the model complexes in these studies have only water-derived ligands. This is not the case for the system discussed in section 3.3, where results obtained for the molecular Co_4-catalyst recently found by Dismukes et al. are discussed.

To obtain results also for the redox steps, the total driving force has to be obtained from experiments. For electrolytic water oxidation carried out at pH = 7, which has a redox potential of 0.82 V, and with a redox potential for the oxidant of 1.29 V (vs NHE),[12] the driving force (in kcal/mol) becomes:

$$\Delta G = 4 \times (0.82 - 1.29) \times 23.06 = -43.4$$

The use of this single experimental value is enough for obtaining the thermodynamics of the redox steps using the computed relative energies, since in the present study we are only interested in the combined release of a (H^+,e^-)-couple. This follows from the fact that the thermodynamics of the reaction

$$2 \times G(H_2O) - 4 \times [E(H^+, e^-) + \text{shift}] \Leftrightarrow G(O_2) + \Delta G$$

is independent of the catalyst. With the explicit values for $G(H_2O)$ = −76.418834 au (gas phase energy + ZPE − 14 kcal/mol), E(H+, e^-) = −0.499972 au (computed as a free hydrogen

dx.doi.org/10.1021/ja4053448 | J. Am. Chem. Soc. 2013, 135, 13804−13813

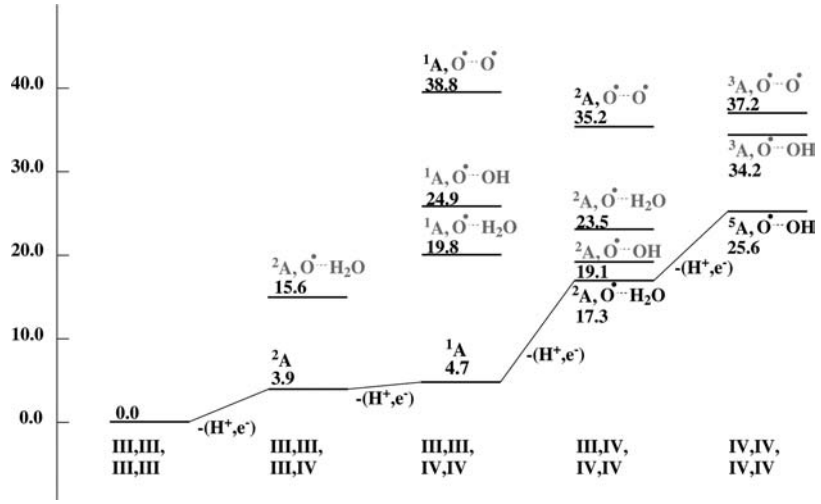

Figure 2. Energy levels for Co_4. Each structure is characterized by its formal oxidation state (at the *x*-axis), its spin-state, and by the number of oxygen-radicals ($O^\bullet$). Only states that are reactive for O−O bond formation are kept in the diagram.

atom), $G(O_2)$ = −150.319980 au (gas phase energy + ZPE − 12 kcal/mol), and the driving force of −43.4 kcal/mol, the shift becomes −92.1 kcal/mol which should be subtracted from the calculated energies for each (H^+,e^-)-couple removed to form a hydrogen atom in gas phase. $G(H^+,e^-)$ is thus equal to $E(H^+,e^-)$ + shift. In comparison to the present system, the corresponding driving force for PSII should be 41.5 kcal/mol computed for the redox potential of P^+_{680} of 1.25 V. However, it was recently realized that the enzyme is able to achieve a higher redox potential of 1.47 V in the last two critical S-transitions, leading to a total driving force of 51.5 kcal/mol.[6]

3.1. The Co_4 Model Complex. The starting point for the discussion of the reactivity of the neutral Co_4 complex is the resting state complex with oxidation states Co_4(III,III,III,III), shown in Figure 1 . This closed shell singlet complex is 44.2 kcal/mol more stable than the corresponding one used in the previous study[25] (the complexes have the same number of oxygens and protons and the same spin). There are many differences between the complexes, one of them being that the present complex has two protonated oxo bridges; the previous one had none. From the present study, the optimal complex without protonated bridges is 22.0 kcal/mol more stable than the one in the previous study. With one protonated bridge, the energy decreases by 13.7 kcal/mol, and with two protonated bridges, the energy goes down a further 8.5 kcal/mol. The energy lowering is due not only to the favorable protonation of the bridges per se, but the accompanying deprotonation of the terminal ligands (to keep the charge neutral) also improves the hydrogen bonding between these ligands.

A significant difference between the present cobalt complexes and the manganese complex in PSII is the optimal spin-state. In the OEC, having mainly carboxylates and oxo ligands, each manganese has a high-spin configuration independent of oxidation state. For the 6-coordinate cobalt complexes, Co(III) and Co(IV) have low-spin ground states, singlet and doublet, respectively, while Co(II) has a high-spin quartet ground state. Forcing Co(III) to be only 5-coordinate changes the preferred spin to be a high-spin triplet, but this coordination has never been found optimal. The complex in Figure 1 thus has a closed shell singlet configuration.

The Co(IV)−$O^\bullet$ state plays a significant role in the discussion below, as a necessary precursor for forming the O−O bond. There are interesting and important electronic structure differences between this state and the Mn(IV)−$O^\bullet$ state, the precursor for O−O bond formation in PSII. In the case of manganese, this state prefers to have the oxygen spin antiparallel to the high-spin coupled spins on the metal leading to a triplet state. The corresponding quintet state, with an oxygen spin parallel to the metal spins, is substantially higher in energy. This is best understood as a mixing with the Mn(V)═O state, which is a triplet in high-spin coupling. The Mn−O bond distance of 1.75 Å, which is shorter than a normal Mn−O single bond of 1.85 Å and longer than a double bond of 1.60 Å, gives further evidence for this mixing. In the case of cobalt, the situation is reversed. The oxygen spin is then strongly preferred to be parallel with the low-spin coupled metal spin, leading to a triplet state. Again, this can be understood as a mixing with the Co(V)═O state which with low-spin coupling is a triplet. The mixing is stronger for cobalt than for manganese with a Co−O bond distance of around 1.65 Å.

The oxidation of the Co_4 complex proceeds by removing (H^+,e^-)-couples. The energy levels reached from the Co_4(III,III,III,III) resting state up to the formal oxidation state Co_4(IV,IV,IV,IV) are shown in Figure 2. The electronic structures are characterized by the number of oxygen radicals ($O^\bullet$) found. A distinction is also made for cases when the donating hydrogen bond to the oxygen radical is coming from an OH or a H_2O. As seen in the diagram the removal of a (H^+,e^-)-couple is endergonic in every step. When the third (H^+,e^-)-couple is removed, the energy, 17.3 kcal/mol, is already so high that an additional O−O bond formation barrier will most probably lead to a very slow reaction.

The first oxidation after the Co_4(III,III,III,III) resting state, with removal of one (H^+,e^-)-couple, leads to formation of a doublet Co_4(III,III,III,IV) state, where the proton removed comes from a bridging hydroxo group. The energy goes up slightly by 3.9 kcal/mol in this transition. The spin is almost entirely located on a cobalt, with a spin-population of 0.93. This result is quite different from a recent study of a Co_4 complex, where DFT calculations using a different functional (PBE0) gave a completely delocalized spin at the same oxidation level.[38] As already indicated in that study, the delocalization could be due to a self-interaction error, which is different for different functionals.[39] None of the present model systems show any

dx.doi.org/10.1021/ja4053448 | J. Am. Chem. Soc. 2013, 135, 13804−13813

delocalization of the type seen in that study. Since the spin is entirely localized on cobalt in the present model, this state is rather unreactive for oxidation of water. The energy required to reach an oxyl radical state is 11.7 kcal/mol and is accompanied by a proton transfer between a terminal hydroxide and a bridging oxyl. From this oxyl radical state, a water attack gives a barrier larger than 25 kcal/mol, which means an overall barrier higher than 40 (3.9 + 11.7 + 25) kcal/mol. The high barrier is partly obtained since the ground spin state for the peroxide product is a quartet Co(II) state. The energy cost is high to force Co(III) to be high spin in the reactant, or Co(II) to be low spin in the product. Spin−orbit coupling would assist in the spin-crossing, but it will not lower the barrier.[37]

With removal of a second (H^+,e^-)-couple the complex reaches the formal Co_4(III,III,IV,IV) state, to the left in Figure 3. Also in this case, a proton is removed from an OH-bridge,

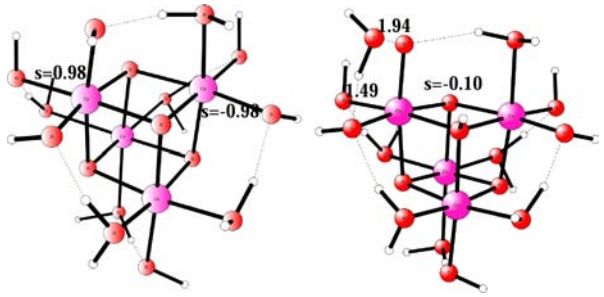

Figure 3. (Left) Optimized structure for the neutral Co_4-model where two of the metals are Co(IV). (Right) Optimized TS-structure with overall barrier of 31.6 kcal/mol.

leading only to unprotonated bridges. The oxidation occurs again for a cobalt rather than for an oxygen ligand, leading to degenerate singlet and triplet states. The energy goes up by another 0.8 kcal/mol in this transition (a total of 4.7 kcal/mol). Also in this case, radical transfer from cobalt to oxygen is necessary for the complex to become reactive for O−O bond formation. In fact, to obtain a sufficiently reactive state, the oxyl radical has to be bound to a Co(IV), leading to a formal Co(V) state. The transitions are here even more energy demanding. The lowest lying singlet and triplet Co_4(III,III,III,IV)−$O^\bullet$ states, are reached at the energies 19.8 and 13.8 kcal/mol, respectively. It should be noted that the lower-lying triplet is not included in Figure 2, since it has a very high barrier for O−O bond formation. In both spin states, the lowest lying degenerate singlet and triplet Co_4(III,III,III,III)−$O^\bullet$−$O^\bullet$ states are found at 38.8 kcal/mol. A state with two oxygen radicals was suggested as the O−O bond-forming state in the previous study[25] but is here found to be too high in energy.

Starting from the formal Co_4(III,III,IV,IV) states with one or more oxyl radicals, there are two possible types of mechanisms. An O−O bond could be formed either by a water attack mechanism or by bond formation with an oxo, another oxyl, or a hydroxyl ligand, a direct coupling (DC) mechanism. In both cases there is a change of spin-states, with the triplet preferred for the reactant and the singlet preferred for the product. Both mechanisms prefer singlet transition states, where the one for the water attack is shown to the right in Figure 3. As seen in the figure, the hydroxyl group is first deprotonated to a bridging oxo, forming a terminal oxyl group. For the singlet Co_4(III,III,III,IV)−$O^\bullet$ state, a water attack on the $O^\bullet$ gives a local barrier of 11.8 kcal/mol. However, since the resting state for this reaction is the Co_4(III,III,III,III) state, which is 19.8 kcal/mol lower in energy, this leads to an overall barrier of 31.6 kcal/mol. The triplet state gives a much higher barrier and is thus unreactive. A direct coupling between $O^\bullet$ and OH^- gives an overall barrier of 34.9 kcal/mol. Water attack is thus the overall preferred pathway at this oxidation level.

The DC and water attack mechanisms are schematically shown for the OEC in PSII in Figure 4 and for the present Co_4

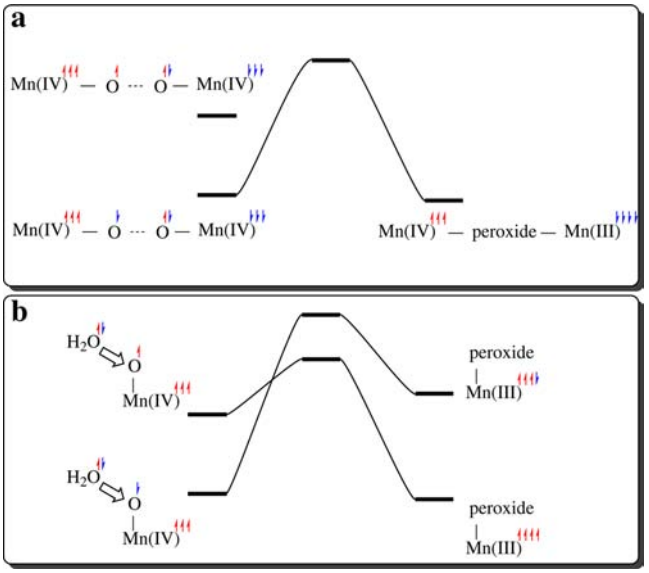

Figure 4. Schematic mechanism for O−O bond formation in PSII; the DC mechanism in a and the water attack mechanism in b.

complexes in Figure 5. For PSII a very low barrier of 11.3 kcal/mol for the DC mechanism was found previously.[5,6] The reason for the low barrier is illustrated in Figure 4a. In the OEC, manganese prefers high-spin coupling of its d-electrons. This means that the reactant Mn(IV) has three parallel d-electrons. Since some mixture of Mn(V)═O is favorable, the oxygen

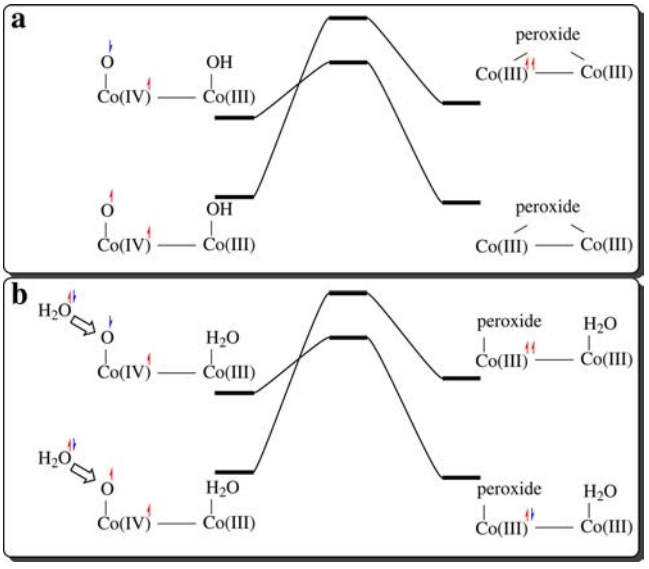

Figure 5. Schematic mechanism for O−O bond formation for Co_4 at the formal (III,III,IV,IV) oxidation level; the DC mechanism in a and the water attack mechanism in b.

dx.doi.org/10.1021/ja4053448 | J. Am. Chem. Soc. 2013, 135, 13804−13813

radical will have a spin which is antiparallel (down-spin) to the manganese spins (up-spins), see above. As the O−O bond forms, a down-spin electron is transferred to the second Mn(IV). Since the product Mn(III) also should be high-spin coupled, its d-electrons have to have down-spins. With this, an electron can flow from one bond to the other without changing its spin, and there will be no spin-crossing when the product (closed shell) peroxide is formed. For the water attack in Figure 4b there is no such possibility, and a spin-crossing is therefore required, leading to a high barrier. For cobalt, the situation is quite different since Co(IV) and Co(III) prefer low-spin coupling. First, for the reactant, a parallel orientation of the oxygen and Co(IV) spins is preferred, in contrast to the case in the OEC, as discussed above. Since the lowest product is a closed shell peroxide, a spin-crossing is required, and the barrier is high, see Figure 5a. For cobalt, the situation is the same for the water attack mechanism as for the DC mechanism, in contrast to the case of manganese. A spin-crossing is required also for the water attack mechanism, and the barrier is high, Figure 5b. In conclusion, the same favorable situation for formation of the O−O bond as found for the OEC in PSII, is in principle not possible for cobalt complexes, unless other ligands can be found which lead to a preference for high-spin rather than low-spin coupling of the d-electrons, or if still another radical is formed, on oxygen or possibly on a ligand. As seen below, an additional oxidation is too costly for the present systems. The arguments given here when comparing cobalt and manganese are similar in spirit to the Woodward−Hoffmann rules in organic chemistry, but use spin instead of orbital symmetry.

The third oxidation after the formal Co_4(III,III,III,III) state, with removal of another (H^+,e^-)-couple, leads to a formal Co_4(III,IV,IV,IV) state. The optimal solution is a degenerate doublet and quartet Co_4(III,III,IV,IV)−$O^\bullet$ states. The energy goes up further by 12.6 kcal/mol in this transition. Note that, for this degenerate doublet state, the component where the metal spins are antiferromagnetically coupled is unreactive for O−O bond formation, since the peroxide formation leads to a high-spin triplet Co(III) state that is high in energy. There is another doublet Co_4(III,III,IV,IV)−$O^\bullet$ state where the metal and the oxygen spins are antiparallel, which is reactive for O−O bond formation but 6.2 kcal/mol higher in energy. The water attack transition state has a local barrier of 12.8 kcal/mol, which means an overall barrier of 36.3 (= 3.9 + 0.8 + 12.6 + 6.2 + 12.8) kcal/mol. By moving one proton from the terminal water ligand to one of the oxo bridges, the degenerate doublet and quartet Co_4(III,III,IV,IV)−$O^\bullet$−$(OH)^-$ states are found. Similar to the above situation, the low-lying doublet has antiferromagnetically coupled metal spins but ferromagnetically coupled metal and oxygen spins. This doublet, however, is reactive for O−O bond formation via either direct coupling or water attack transition states, found at energies of 34.2 kcal/mol for direct coupling and of 36.1 kcal/mol for the water attack. The Co_4(III,III,IV,IV)−$O^\bullet$−$O^\bullet$ state can be obtained by further proton rearrangement but lies much higher in energy.

A fourth oxidation after the formal Co_4(III,III,III,III) state, with removal of another (H^+,e^-)-couple, leads to a formal quintet Co_4(IV,IV,IV,IV) state. The energy goes up by another 8.3 kcal/mol. The degenerate singlet and triplet states, which are reactive for O−O bond formation at this stage, are more than 8.7 kcal/mol higher than the quintet ground state, which essentially excludes this transition.

In summary, the lowest barrier obtained for the neutral Co_4 model complex is 31.6 kcal/mol for a water attack with the formal Co_4(III,III,IV,IV) state. This is considerably higher than the barrier for the amorphous experimental system of 21.8 kcal/mol (calculated from TS-theory) and indicates that there are differences between the amorphous system and the present Co_4 model. The corresponding computed barrier for PSII is 11.3 kcal/mol.[6]

3.2. Co_3, Co_5 and Larger Model Complexes. In order to investigate the role of possible defects for cobalt−oxo complexes, the water oxidation activity was also studied for Co_3 and Co_5 models, where one cobalt was either removed or added. As for the Co_4 complex, each cobalt is 6-coordinate, and the number of protons have been adjusted to keep the cluster neutral. An energy diagram, similar to the one discussed above for Co_4 was constructed also for Co_3, see Figure 6. Starting with

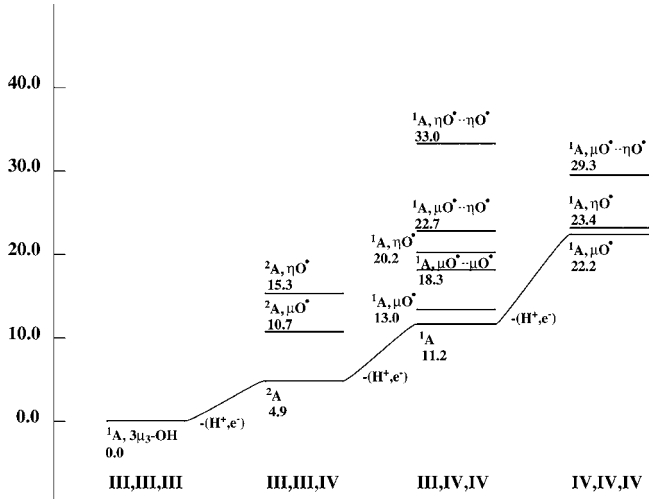

Figure 6. Energy levels for Co_3. Each structure is characterized by its formal oxidation state (at the *x*-axis), its spin-state, and by the number of oxygen radicals ($O^\bullet$). Only states that are reactive for O−O bond formation are kept in the diagram.

the closed shell singlet Co_3(III,III,III) state, the first step is a removal of a (H^+,e^-)-couple to reach a formal doublet Co_3(III,III,IV) state, 4.9 kcal/mol higher in energy. This state has one Co(IV). The lowest active complex is obtained for a bridging oxyl radical coupled to a Co_3(III,III,III) state at 10.7 kcal/mol. The state with a terminal oxyl radical instead is 4.6 kcal/mol higher. Again, as in the Co_4 case, this state with only one formal Co(IV) is unreactive. The water attack has a barrier of over 30 kcal/mol, and that for the DC mechanism is even higher. With another (H^+,e^-)-couple removed, the energy goes up to 11.2 kcal/mol, and a formal Co_3(III,IV,IV) state is reached. The lowest active formal Co(V) state with one bridging oxyl radical is at an energy of 13.0 kcal/mol. For the water attack mechanism the local barrier from the Co_3(III,IV,IV) singlet reactant is 16.1 kcal/mol, leading to an overall barrier of 27.3 (16.1 + 11.2) kcal/mol. The transition state is shown to the left in Figure 7. For the DC case, two bridging oxyl radicals are involved with an overall barrier of 31.6 kcal/mol, to the right in Figure 7. The lowest barrier for Co_3 is thus not too different from the Co_4 case, but somewhat lower with 27.3 kcal/mol compared to 31.6 kcal/mol. The conclusion is that the Co_3-model, which should represent a

dx.doi.org/10.1021/ja4053448 | J. Am. Chem. Soc. 2013, 135, 13804−13813

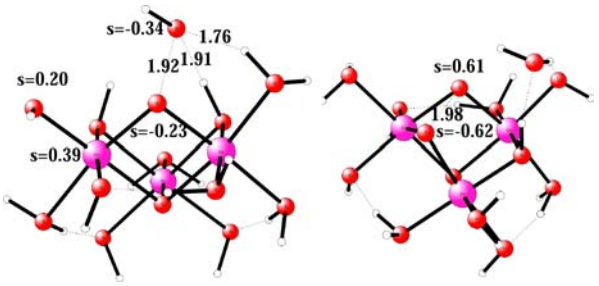

Figure 7. Optimized TS-structures for water attack for Co_3, to the left, and for direct O−O coupling, to the right.

defect of the perfect crystal, lowers the barrier but not as dramatically as one might have expected.

The Co_3 mechanism was followed through the full cycle. The release of O_2 is a rather complicated process with several steps. In the first step, a superoxide radical is formed. At that stage, the spin-distribution becomes very complicated. One cobalt with spin s = 1.79 can be described as a triplet Co(III) state. A second cobalt has spin s = 2.72 and is therefore a quartet Co(II), while the third cobalt has no spin and is thus a clean Co(III) state. One spin resides on the superoxide radical, which means that there are a total of about six unpaired spins, which would correspond to a septet state if ferromagnetic coupling had been used.

In the next step a water molecule becomes bound to the Co(II) cobalt. The superoxide remains the same as do the spins on cobalt. The barrier is 12.5 kcal/mol with respect to the resting reactant. In the final, third step of O_2 release, there is an early TS with similar spins as in the previous steps, except that there is an antiferromagnetic coupling between O_2 and the Co(III) cobalt. The barrier for this step is 13.4 kcal/mol. The product can be described as a Co_3(III,II,II) state with a free triplet O_2. To return to the resting Co_3(III,III,III) state, one water needs to be added, and two (H^+,e^-)-couples need to be removed. These two steps are quite exergonic with −25.0 and −15.7 kcal/mol, respectively. The energy diagram is shown in Figure 8.

Isotope-labeling experiments have been done for the Nocera catalyst, with labeled oxygens in the catalyst and unlabeled oxygens in the water solvent.[12] It is found that most O_2 initially released has unlabeled oxygens from the solvent water. It is also known that the oxygens bound as oxo groups in the catalyst only exchange with the surrounding water at a very slow time-scale, much slower than that of oxygen evolution. This best fits a water attack mechanism for the initial O_2 release. After a while, labeled oxygens from the cobalt−oxide catalyst start to appear in O_2. With mixed labels, this should come from a water attack mechanism involving a bridging oxo group. If both oxygens are labeled this fits best with a DC mechanism. However, since oxygen exchange between the solvent and the catalyst could not be ruled out at the time scale of the experiments, conclusions are not easily drawn from these experiments. It has also been found that the catalyst is rather quickly broken down.[12] Using Co_3 as a model, it is straightforward to understand why. In the DC mechanism, removal of the peroxide in the cluster leads to very large structural changes. For the water attack mechanism the water attack is on a bridging oxyl radical which also severely disrupts the cluster. Since for the Co_4 cluster the water attack is on a terminal oxyl radical, the distortions should be much less dramatic.

It was finally tested if a lower barrier could be obtained by charging the complex. The complexes described above are all neutral. A proton was first added to create a positive complex. This led to an increased energy cost for the two steps when the cluster is oxidized to reach the active redox level. This extra cost remains when the O−O bond is formed and the added proton

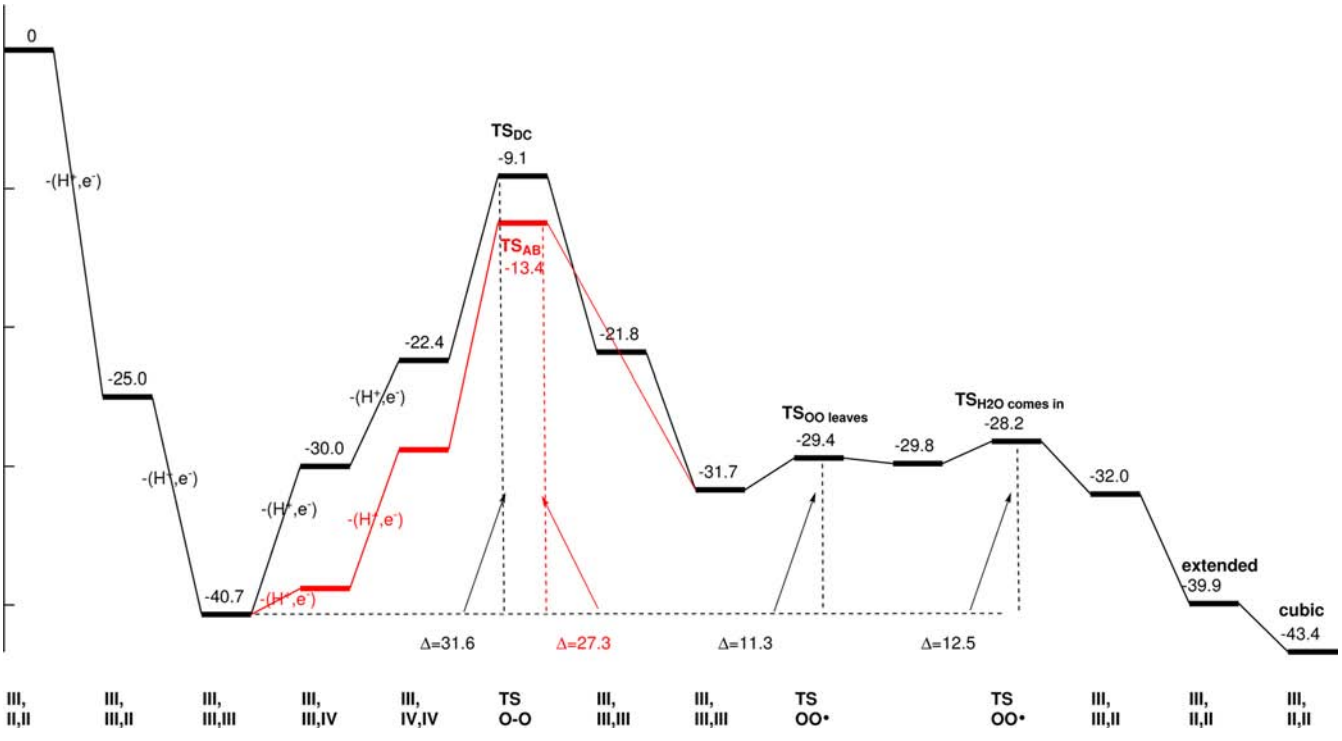

Figure 8. Energy diagram for the full water oxidation cycle with the Co_3 model complex.

dx.doi.org/10.1021/ja4053448 | J. Am. Chem. Soc. 2013, 135, 13804−13813

is therefore no advantage for water oxidation. For a negative complex where one proton is removed, a barrier of 27.1 kcal/mol was obtained. This is almost identical to the one for the neutral complex of 27.3 kcal/mol. No advantage of charging the complex has therefore been found.

Some Co_5 model complexes were also studied, with structural details shown as Supporting Information The most straightforward way to place a fifth Co(III) on the optimal Co_4(III,III,III,III) complex is to put it on in a way that modifies the Co_4 complex as little as possible. This leads to a complex where three ligands are shared. After minor proton rearrangements the lowest energy structure was obtained. When only the Co_4 part is oxidized twice, the energy goes up by 9.8 kcal/mol, compared to 4.7 kcal/mol for the bare Co_4 complex, see above. The total barrier for O−O bond formation (of a type similar to that for the Co_4 complex) lies at 33.1 kcal/mol, which is actually somewhat higher than for Co_4 at 31.6 kcal/mol. Some searches (based on the experience from Co_4) for lower transition states were made, but no lower barrier was found. A different type of Co_5 complex was also tried, where the fifth cobalt only shares two ligands with the Co_4 part. The optimal complex of this type is 15.4 kcal/mol higher in energy than the one with three shared ligands. However, from this point the total barrier for water attack is only 24.7 kcal/mol, which could have some bearing on larger clusters.

Some Co_8 complexes were also investigated; the first one was with linearly connected Co_4 cubes. Surprisingly, if the two oxidations are restricted to the central cube, the energy goes up by as much as 48.8 kcal/mol. The reason is probably the presence of μ_4-O bridges on the central cube, which are much less negative and therefore do not stabilize the required formal Co(V) state.

3.3. The Dismukes Co_4 Complex. As mentioned in the Introduction, Dismukes et al. have reported water oxidation activity for the molecular catalyst $Co_4O_4(OAc)_4(py)_4$, with a rate that corresponds to a barrier of about 20.0 kcal/mol (using TS theory).[16] It should be noted that this is for a redox potential of 1.43 V of the oxidant, higher than the one used for the Nocera-type complexes of 1.29 V. The catalytic pathway was here studied only in the steps from Co_4(III,III,III,III) to Co_4(III,III,IV,IV). At the formal Co_4(III,III,III,IV) level, one cobalt is oxidized, and a proton is released from a water molecule entering from the bulk. This leads to a terminally bound hydroxyl ligand. At the formal Co_4(III,III,IV,IV) level, the oxidation is followed by another proton release, giving a reactive terminal oxyl radical with its spin antiparallel to the spin on the Co(IV) it binds to. As, discussed above, this is the singlet excited state of a formal Co(V) state. The state where the oxygen spin is parallel to the Co(IV) spin is 5.6 kcal/mol lower in energy but it is unreactive. Other geometries with two hydroxyl ligands instead of one oxo ligand have been tried, but all lie higher in energy. The structural conformation does not allow a favorable O−O direct coupling mechanism, and a water attack mechanism is therefore preferred. The water is deprotonated by an OAc^- ligand, and the critical O−O bond length is 2.12 Å (see Figure 9 to the left). The barrier for the single step of water attack is 14.4 kcal/mol. However, just as for the Nocera-type catalysts discussed in the previous sections, the Co_4(III,III,III,III) solution is the lowest energy species on the potential energy surface. With a redox potential of 1.43 V, as used in the experiments, the overall barrier for O−O bond formation is calculated to be 23.0 kcal/mol. From the study of the full catalytic cycle for Co_3, it can safely be assumed that the steps following O−O bond formation are not rate limiting. This means that the calculated barrier is in good agreement with the experimental barrier of 20.0 kcal/mol.

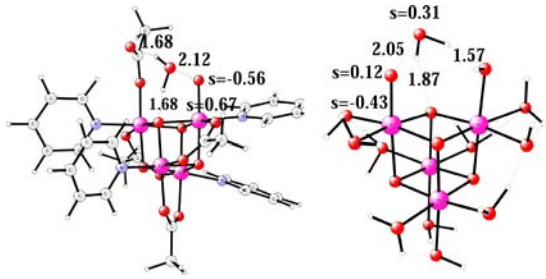

Figure 9. Optimized TS-structures for water attack for the Dismukes complex, to the left, and for the water and hydroxide substituted structure to the right.

The barrier for the Dismukes complex is thus substantially lower than for the Co_4 model discussed above for the Nocera-type complex with 31.6 kcal/mol. However, the difference in redox potential is very important in this context. This difference of 0.14 V (3.2 kcal/mol) leads to an advantage every time a (H^+,e^-)-couple is released. Two of these releases are part of the height of the barrier. Assuming that all of this energy is used for (H^+,e^-) release, the barrier for the Dismukes complex would increase if the lower redox potential was used by 2 × 3.2 to 29.4 kcal/mol, only 2.2 kcal/mol lower than for the Nocera-type Co_4 complex of 31.6 kcal/mol. Still, the difference of 2.2 kcal/mol corresponds to more than 1 order of magnitude in rate and further investigations of this difference was therefore performed. The origin of this difference could, of course, be the different ligands used but also the difference in protonation of the oxo groups. In the Dismukes complex all oxo groups are unprotonated, while in the best model of the Nocera-type Co_4 complex two oxo groups are protonated. To make the systems more similar, the OAc^- in the Dismukes complex was substituted by a water−hydroxide pair and py with a water, without further redistribution of protons in contrast to what was done for the Nocera-type complex. As a result, there are water−hydroxide hydrogen-bonding pairs on four of the six cubic faces. The other two faces have two water molecules that are not hydrogen-bonded to each other. The structures are optimized from Co_4(III,III,III,III) to Co_4(III,III,IV,IV). During the oxidations, a water molecule is deprotonated to form an oxyl radical with its spin antiparallel to the one on Co(IV), exactly as for the complex with the real ligands. The water attack transition state, shown to the right in Figure 9, has an O−O bond length of 2.05 Å . The barrier of this single step is 13.0 kcal/mol. With the redox potential used for the Dismukes complex of 1.43 V, the overall barrier should be 25.2 kcal/mol. With the lower redox potential of 1.29 V the barrier becomes 31.6 kcal/mol, in exact agreement with the one for the Nocera-type complexes discussed above. The electronic configuration is also the same for the two types of complexes. The protonation states of the oxo ligands, therefore, do not seem to affect the rate. Subtle differences in the character of the ligands are instead the probable reasons for the 2.2 kcal/mol lower barrier height for the Dismukes complex.

4. CONCLUSIONS

Water oxidation mechanisms have been studied for a large number of different cobalt complexes, most of them with four cobalt atoms. For the only system for which the structure has

dx.doi.org/10.1021/ja4053448 | J. Am. Chem. Soc. 2013, 135, 13804−13813

been experimentally determined, the Dismukes complex,[16] the calculated barrier is in good agreement with the measured one, 23.0 compared to 20.0 kcal/mol. For all systems studied here, a redox level with two Co(IV) (the rest Co(III)), is the lowest level where water oxidation activity is significant. Furthermore, a state with an oxygen radical coupled to a Co(IV) state, a formal Co(V) state, is needed for reactivity, which often requires appreciable additional excitation from the corresponding state with two Co(IV) centers. The best mechanism found is a water attack on the oxygen radical. For the Dismukes complex, the endergonic release of two (H^+,e^-)-couples is needed to reach the active redox level. This means that this endergonicity will be part of the rate-limiting barrier. While the local O−O bond formation step is not helped in a significant way by an oxidant with a high redox potential, the release of (H^+,e^-)-couples is. The redox potential of the oxidant used for the Dismukes complex is 1.43 V.

To analyze the reactivity of the amorphous cobalt complexes by Nocera et al, a simple model was used with only water derived ligands. This type of model has been used before,[25] with quite different results than the ones obtained here. For the Co_4 model complex a high barrier of 31.6 kcal/mol was found here for a mechanism very similar to the one found for the Dismukes complex. This barrier for the Nocera-type complex may thus appear to be much higher than the one of 23 kcal/mol for the Dismukes complex, but that one was obtained for a higher redox potential of 1.43 V. If the barriers are transformed to the same redox potential of 1.29 V and assuming that all of the difference in redox potential is used for (H^+,e^-) release, the barriers for the two types of systems are much more similar, differing by only 2.2 kcal/mol. The effect of the higher redox potential is not obvious without a detailed mechanism at hand, but depends on how many releases of (H^+,e^-)-couples are part of the rate-limiting barrier, and could in principle have given a zero effect.

Since the lowest barrier obtained for the present Co_4 models of the Nocera complex is much higher than the one measured for the amorphous system, 31.6 kcal/mol compared to 21.8 kcal/mol, additional investigations were done. Co_3 and Co_5 models, and some larger ones, were taken as examples of more irregular structures where defects and edges might show effects on the water oxidation rates. The Co_3 complexes were studied in as much detail as the Co_4 complexes, but only small defect or edge effects were found, lowering the barrier to 27.3 kcal/mol. Perhaps, more irregular structures might appear for even larger clusters. Alternatively, the rather low barrier obtained for the Nocera catalyst, might be due to the presence of other types of atoms in the clusters, like alkali atoms, which could have effects as dopants. The phosphates in the catalyst are not believed to be significant for the water oxidation mechanism.[26] Another possibility might be that the more accessible electrons for a larger system would allow still another local (H^+,e^-) release, making the final O−O bond formation even easier. An entirely different mechanism, not involving an oxyl radical, is at the present stage considered very unlikely. It should perhaps finally be mentioned that there are as yet some uncertainties concerning the experimental rate. Dau et al have given a rate of 0.2 s^{-1} with a higher redox potential of 1.45 V,[40] corresponding to a barrier of 18.6 kcal/mol. At 1.45 V, our computed barrier for the Co_3 complex is 20.4 kcal/mol, which is actually quite close to the one given by Dau et al.

The most important conclusion drawn here concerns the intrinsic difference between manganese and cobalt clusters as water oxidation catalysts. For the manganese cluster in PSII, a very efficient direct coupling mechanism is possible, see Figure 4, which is not possible for cobalt clusters of the type studied here, see Figure 5. This difference is due to the different type of optimal spin coupling. Manganese prefers high-spin coupling which allows a smooth formation of the O−O bond from the oxyl reactant to the peroxide product. Cobalt, on the other hand, prefers low-spin coupling for the relevant high oxidation states, which forces a costly change of electronic structure during the formation of the O−O bond.

■ ASSOCIATED CONTENT

Ⓢ Supporting Information

Coordinates for the structures in the figures and diagrams. This material is available free of charge via the Internet at http://pubs.acs.org.

■ AUTHOR INFORMATION

Corresponding Author

ps@organ.su.se

Notes

The authors declare no competing financial interest.

■ ACKNOWLEDGMENTS

We are grateful to the Trygger Foundation for financing the Postdoc-Fellowship for X.L.

■ REFERENCES

(1) Ferreira, K. N.; Iverson, T. M.; Maghlaoui, K.; Barber, J.; Iwata, S. *Science* **2004**, *303*, 1831−1838.
(2) Guskov, A.; Kern, J.; Gabdulkhakov, A.; Broser, M.; Zouni, A.; Saenger, W. J. *Nat. Struct. Biol.* **2009**, *16*, 334−341.
(3) Umena, Y.; Kawakami, K.; Shen, J.-R.; Kamiya, N. *Nature* **2011**, *473*, 55−60.
(4) Siegbahn, P. E. M. *Chem.—Eur. J.* **2008**, *27*, 8290−8302.
(5) Siegbahn, P. E. M. *Chem.—Eur. J.* **2006**, *12*, 9217−9227.
(6) Siegbahn, P. E. M. *Biochim. Biophys. Acta* **2013**, *1827*, 1003−1019.
(7) Ames, W. M.; Pantazis, D. A.; Krewald, V.; Cox, N.; Messinger, J.; Lubitz, W.; Neese, F. *J. Am. Chem. Soc.* **2011**, *133*, 19743−19757.
(8) Rapatskiy, L.; Cox, N.; Savitsky, A.; Ames, W. M.; Sander, J.; Nowacyzk, M. M.; Rögner, M.; Boussac, A.; Neese, F.; Messinger, J.; Lubitz, W. *J. Am. Chem. Soc.* **2012**, *134*, 16619−16634.
(9) Grundmeier, A.; Dau, H. *Biochim. Biophys. Acta* **2012**, *1817*, 88−105.
(10) Renger, G. *Biochim. Biophys. Acta* **2012**, *1817*, 1164−1176.
(11) Gatt, P.; Stranger, R.; Pace, R. J. *J. Photochem. Photobiol. B* **2011**, *104*, 80−93.
(12) Kanan, M. W.; Nocera, D. G. *Science* **2008**, *321*, 1072. Nocera, D. G. *Acc. Chem. Res.* **2012**, *45*, 767−776. Surendranath, Y.; Kanan, M. W.; Nocera, D. G. *J. Am. Chem. Soc.* **2010**, *132*, 16501−16509.
(13) Risch, M.; Khare, V.; Zaharieva, I.; Gerencser, L.; Chernev, P.; Dau, H. *J. Am. Chem. Soc.* **2009**, *131*, 6936−6397.
(14) Kanan, M. W.; Yano, J.; Surendranath, Y.; Dinca, M.; Yachandra, V. K.; Nocera, D. G. *J. Am. Chem. Soc.* **2010**, *132*, 13692−13701.
(15) Jiao, F.; Frei, H. *Angew. Chem., Int. Ed.* **2009**, *48*, 1841.
(16) McCool, N. S.; Robinson, D. M.; Sheats, J. E.; Dismukes, C. *J. Am. Chem. Soc.* **2011**, *133*, 11446−11449.
(17) Gardner, G. P.; Bok, Go, Y.; Robinson, D. M.; Smith, P. F.; Hadermann, J.; Abakumov, A.; Greenblatt, M.; Dismukes, C. *Angew. Chem., Int. Ed.* **2012**, *51*, 1616−1619.
(18) Artero, V.; Chavarot-Kerlidou, M.; Fontecave, M. *Angew. Chem., Int. Ed.* **2011**, *50*, 7238−7266.
(19) McAlpin, J. G.; Stich, T. A.; Casey, W. H.; Britt, R. D. *Coord. Chem. Rev.* **2012**, *256*, 2445−2452.

(20) Gilbert, J. A.; Eggleston, D. S.; Murphy, W. R.; Geselowitz, D. A.; Gersten, S. W.; Hodgson, D. J.; Meyer, T. J. *J. Am. Chem. Soc.* **1985**, *107*, 3855−3864.
(21) Sala, X.; Romero, I.; Rodriguez, M.; Escriche, L.; Llobet, A. *Angew. Chem., Int. Ed.* **2009**, *48*, 2842−2852.
(22) Li, X.; Chen, G.; Schinzel, S.; Siegbahn, P. E. M. *Dalton Trans.* **2011**, *40*, 11296−11307.
(23) Nyhle'n, J.; Duan, L.; Åkermark, B.; Sun, L.; Privalov, T. *Angew. Chem., Int. Ed.* **2010**, *49*, 1773−1777.
(24) Du, P. W.; Eisenberg, R. *Energy Environ. Sci.* **2012**, *5*, 6012−6021.
(25) Wang, L. P.; Van Voorhis, T. *J. Phys. Chem. Lett.* **2011**, *2*, 2200−2204.
(26) Dinca, M.; Surendranath, Y.; Nocera, D. G. *Proc. Natl. Acad. Sci. U.S.A.* **2010**, *107*, 10337−10341.
(27) Siegbahn, P. E. M. *J. Am. Chem. Soc.* **2009**, *131*, 18238−18239.
(28) Siegbahn, P. E. M. *Acc. Chem. Res.* **2009**, *42*, 1871−1880.
(29) Siegbahn, P. E. M.; Blomberg, M. R. A. In *Computational Modeling for Homogeneous Catalysis and Biocatalysis*; Morokuma, K., Musaev, J., Eds.; Wiley-VCH: Weinheim, Germany, 2008; pp 57−81.
(30) Rossmeisl, J.; Dimitrievski, K.; Siegbahn, P.; Nørskov, J. K. *J. Phys. Chem. C* **2007**, *111*, 18821−18823.
(31) Reiher, M.; Salomon, O.; Hess, B. A. *Theor. Chem. Acc.* **2001**, *107*, 48−55.
(32) *Jaguar* 7.9; Schrödinger, LLC: Portland, OR, 1991−2013.
(33) Frisch, M. J.; Trucks, G. W.; Schlegel, H. B.; Scuseria, G. E.; Robb, M. A.; Cheeseman, J. R.; Scalmani, G.; Barone, V.; Mennucci, B.; Petersson, G. A.; Nakatsuji, H.; Caricato, M.; Li, X.; Hratchian, H. P.; Izmaylov, A. F.; Bloino, J.; Zheng, G.; Sonnenberg, J. L.; Hada, M.; Ehara, M.; Toyota, K.; Fukuda, R.; Hasegawa, J.; Ishida, M.; Nakajima, T.; Honda, Y.; Kitao, O.; Nakai, H.; Vreven, T.; Montgomery, J. A., Jr.; Peralta, J. E.; Ogliaro, F.; Bearpark, M.; Heyd, J. J.; Brothers, E.; Kudin, K. N.; Staroverov, V. N.; Kobayashi, R.; Normand, J.; Raghavachari, K.; Rendell, A.; Burant, J. C.; Iyengar, S. S.; Tomasi, J.; Cossi, M.; Rega, N.; Millam, N. J.; Klene, M.; Knox, J. E.; Cross, J. B.; Bakken, V.; Adamo, C.; Jaramillo, J.; Gomperts, R.; Stratmann, R. E.; Yazyev, O.; Austin, A. J.; Cammi, R.; Pomelli, C.; Ochterski, J. W.; Martin, R. L.; Morokuma, K.; Zakrzewski, V. G.; Voth, G. A.; Salvador, P.; Dannenberg, J. J.; Dapprich, S.; Daniels, A. D.; Farkas, O.; Foresman, J. B.; Ortiz, J. V.; Cioslowski, J.; Fox, D. J. *Gaussian 09*, Revision A.1; Gaussian, Inc.: Wallingford CT, 2009.
(34) Bediako, D. K.; Surendranath, Y.; Nocera, D. G. *J. Am. Chem. Soc.* **2013**, *135*, 3662−3674.
(35) Siegbahn, P. E. M.; Blomberg, M. R. A.; Chen, S.-L. *J. Chem. Theory Comput.* **2010**, *6*, 2040−2044.
(36) Grimme, S. *J. Chem. Phys.* **2006**, *124*, 034108. Schwabe, T.; Grimme, S. *Phys. Chem. Chem. Phys.* **2007**, *9*, 3397−3406.
(37) Lundberg, M.; Siegbahn, P. E. M. *Chem. Phys. Lett.* **2005**, *401*, 347−351.
(38) McAlpin, J. G.; Stich, T. A.; Ohlin, C. A.; Surendranath, Y.; Nocera, D. G.; Casey, W. H.; Britt, R. D. *J. Am. Chem. Soc.* **2011**, *133*, 15444−15452. McAlpin, J. G.; Surendranath, Y.; Dinca, M.; Stich, T. A.; Stoian, S. A.; Casey, W. H.; Nocera, D. G.; Britt, R. D. *J. Am. Chem. Soc.* **2010**, *132*, 13692.
(39) Lundberg, M.; Siegbahn, P. E. M. *J. Chem. Phys.* **2005**, *122*, 224103−1−9.
(40) Dau, H.; Limberg, C.; Reier, T.; Risch, M.; Roggan, S.; Strasser, P. *ChemCatChem.* **2010**, *2*, 724−761.